THE TORSIONAL BEHAVIOUR OF TRIANGULAR STRAND STEEL WIRE ROPES FOR DRUM WINDERS

Gerhard Rebel

A thesis submitted to the Faculty of Engineering, University of the Witwatersrand, in fulfilment of the requirements for the degree of Doctor of Philosophy.

Johannesburg
1997

3.2 Torque-tension machine description

3.2.1 General layout

Figures 3.2 and 3.3 show the layout of the main components of the torque-tension machine. The hydraulic cylinder provides the axial load and the motor, with a reduction drive, can twist up or untwist the specimen as required. The scissor mechanism at the rear of the hydraulic cylinder, figure 3.4, allows axial movement but prevents rotation of the cylinder shaft. The measurement specifications of the machine are listed in table 3.1. The overall accuracies of the measurement systems were determined during the development project and represent the worst cases. They include nonlinearity, hysteresis, temperature effects and the data acquisition system resolution.

Table 3.1 - Measurement specifications of the tension-torsion testing machine.

Measurement parameter	**Allowable range**	**Overall accuracy**
Load	$0 \rightarrow 500$ kN	$\pm$ 1.8 kN full scale
Torque	$-3200 \rightarrow +3200$ Nm	$\pm$ 4.9 Nm full scale
Elongation	$-130 \rightarrow +130$ mm	$\pm$ 1.3 mm full scale
Diameter change	$-5 \rightarrow +5$ mm	$\pm$ 0.03 mm full scale
End rotation	$-700 \rightarrow +700$ turns	$\pm$ 1.0° (backlash in the reduction drive)

Rope diameters up to 64 mm can be accommodated. Depending on the construction, the maximum load may need to be limited so as not to exceed the torque limits of the loadcell.

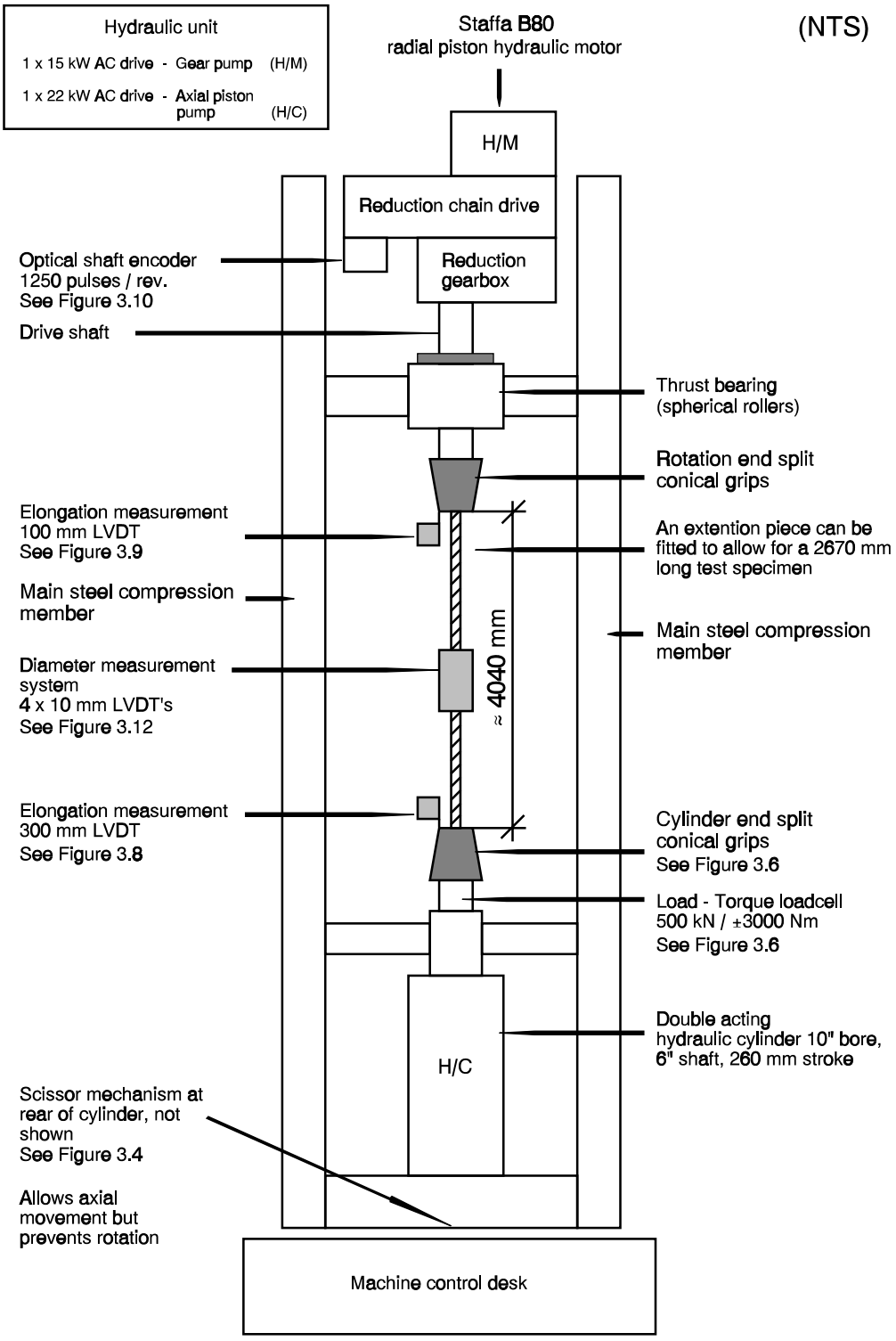

Figure 3.2 - General arrangement of the steel wire rope torque-tension testing machine.

Figure 3.3 - View of the steel wire rope torque-tension testing machine. The entire machine operation is controlled by the PC in the foreground.

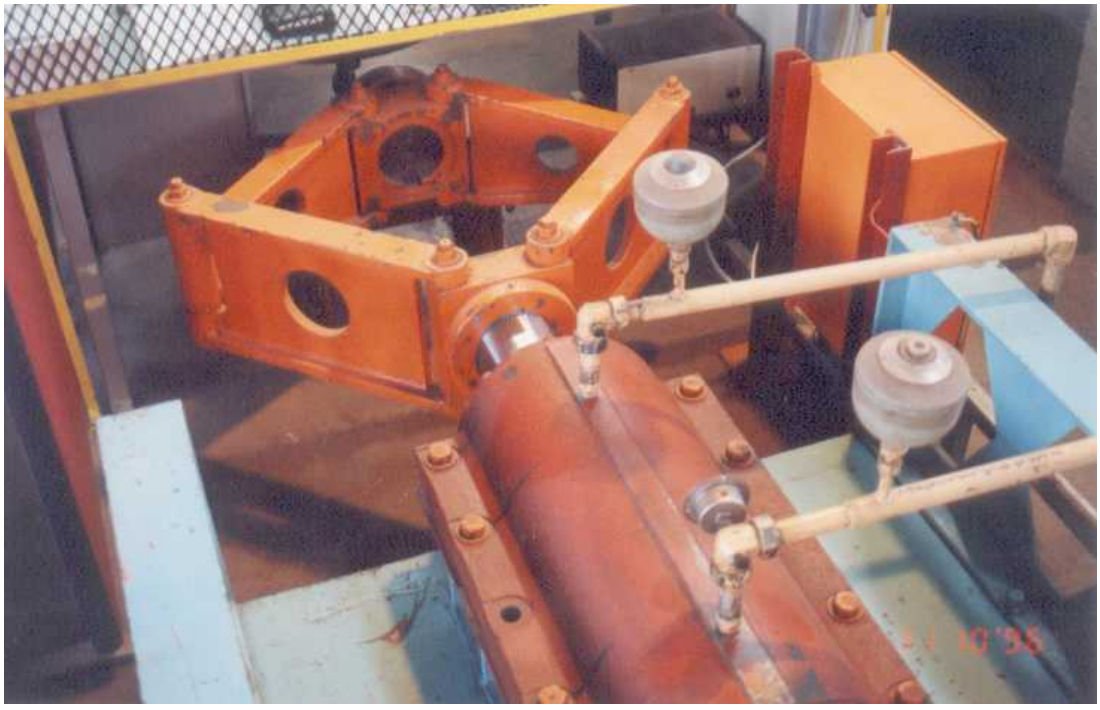

Figure 3.4 - View of the scissor mechanism at the rear of the hydraulic cylinder (orange linkage arrangement). Rotation of the cylinder shaft is prevented while allowing axial movement

3.2.2 Electrical and hydraulic control system

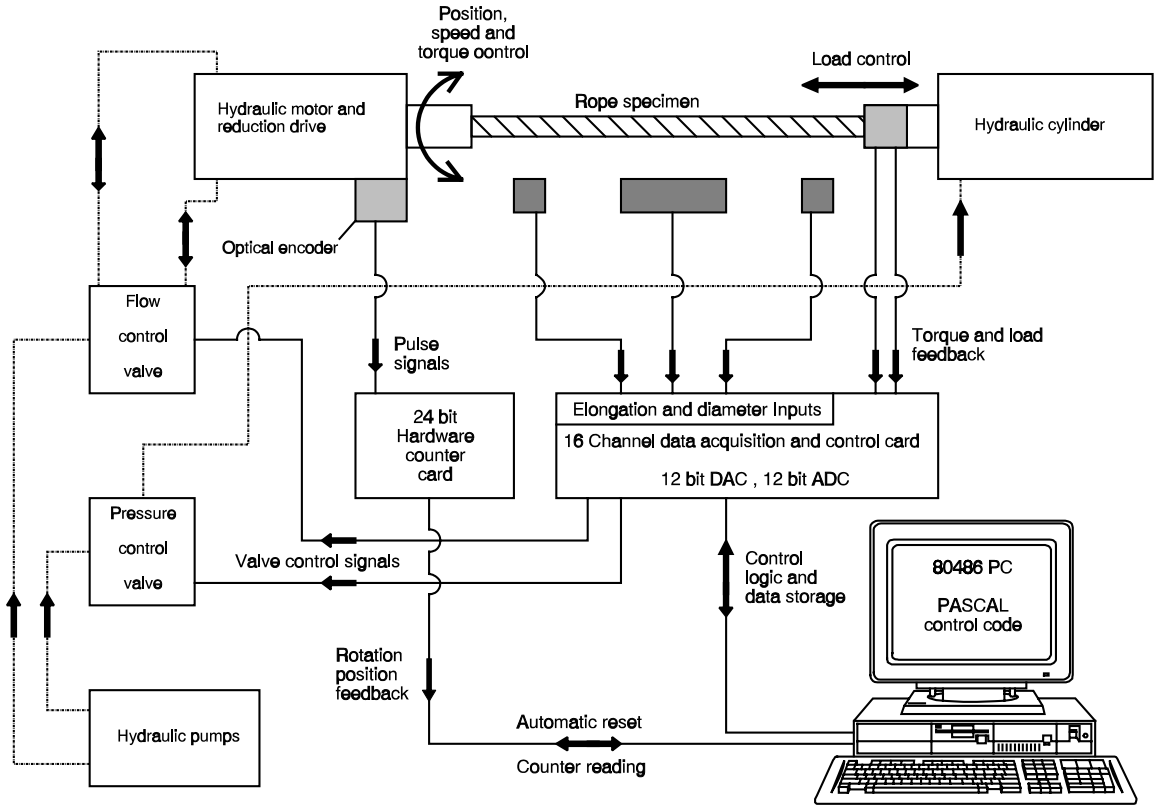

Figure 3.5 - Basic configuration of the machine control system.

Closed loop control of rope load, torque and end rotation is achieved with the system shown in figure 3.5. PASCAL control and data acquisition software provides the machine - operator interface. Proportional pressure relief and flow control valves are used to vary the rope load and end rotation respectively. It was originally anticipated that an electromechanical brake may be required to hold the rotation end drive shaft (figure 3.2) in a fixed position during testing. This was however not necessary as the software control of the five cylinder radial piston motor resulted in an angular position error of less than 1°.

3.2.3 Load and torque measurement

A combination load-torque load cell is used to measure the rope load and torque simultaneously. Two strain gauge bridges (full) are applied to a heat treated En30B circular shaft with end fittings which connect to the hydraulic cylinder and the split

conical grips. Mounting of the load cell directly behind the grips on the cylinder end, figure 3.6, eliminates measurement errors due to the shaft bearing friction. During the dead weight calibration of the load cell, the cross load and cross torque outputs of the bridges are taken into account in determining the overall accuracy. The bridges are fitted with shunt resistances for in-situ calibration of the load and torque outputs. The mechanical equivalence of the shunt induced imbalance was determined during the dead weight calibration procedures.

Figure 3.6 - View of the load cell (white cylindrical section) installed between the cylinder shaft and the conical rope grips. The rope specimen is to the right and the shaft bearing arrangement is on the extreme left.

3.2.4 Elongation measurement

Rope specimen elongation, as a result of loading and changes in the state of twisting, is measured by two Linear Variable Differential Transformers (LVDT) mounted on support pedestals bolted to the laboratory floor. The general arrangement of the LVDT's is shown in figure 3.7 with detail of the cylinder and rotation ends contained in figures 3.8 and 3.9. When the system was first installed elongation was determined using equation [3.1].

$$\Delta l = \Delta \text{ LVDT}_{\text{Cylinder End}} + \Delta \text{ LVDT}_{\text{Rotation End}} \qquad [3.1]$$

However, it was discovered that there was an error in the elongation value depending on the position of the rotation head, figure 3.9. The rotation end split collar clamp is attached to the cast white metal collar of the rope and is therefore unlikely to be perfectly perpendicular to the axis of rotation. The result is a sinusoidal oscillation of the rotation end LVDT plunger which gives rise to the error in the reading. To overcome the problem the software executes a check, at constant load, to determine the magnitude of the sinusoidal displacement for angles between -180° to +180°. During testing, equation [3.2] is used to accurately determine the rope elongation.

$$\Delta l = \Delta \text{LVDT}_{\text{Cylinder End}} + \Delta \text{LVDT}_{\text{Rotation End}} - \text{skewness factor} \qquad [3.2]$$

The skewness factor is interpolated from a look up table created during the skewness check and is a function of the current angle of rotation. The look up table is valid for all angles since any angle ϕ can be converted to an angle $ß$ between -180° and +180° using equation [3.3]. The gauge length (l_0) of the specimen is determined by measuring the distances *x* and *y* and adding these to the fixed length between the measurement pedestals, figure 3.7.

$$ß = (\phi/360 - \text{round}(\phi/360 - 1) - 1).360 \qquad [3.3]$$

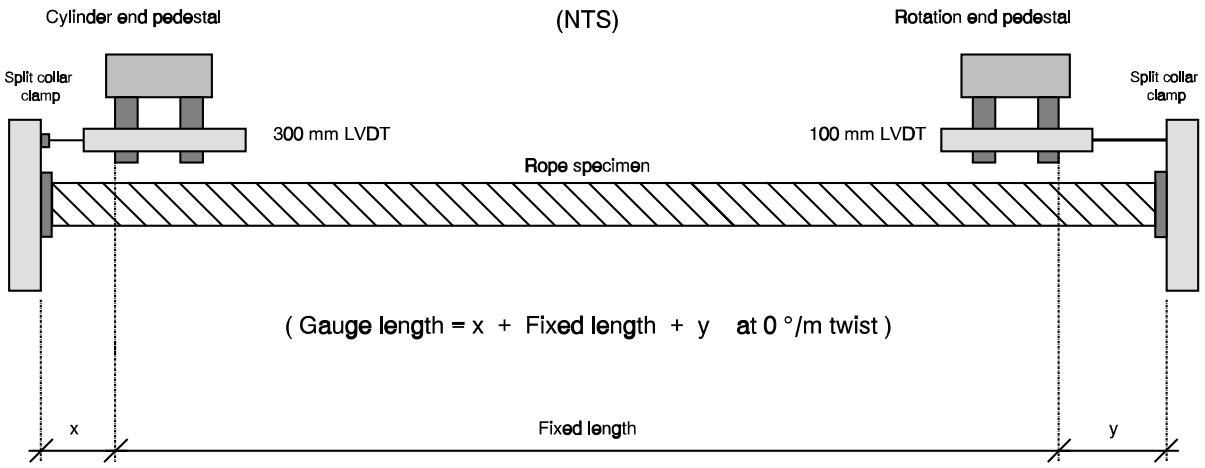

Figure 3.7 - Arrangement of the rope elongation measurement system hardware.

Figure 3.8 - Tension cylinder end, LVDT configuration. The magnet ensures that the LVDT plunger follows the split collar clamp movement and allows for simple connection during the rope installation. Sprung LVDT's of 300 mm stroke are not readily available.

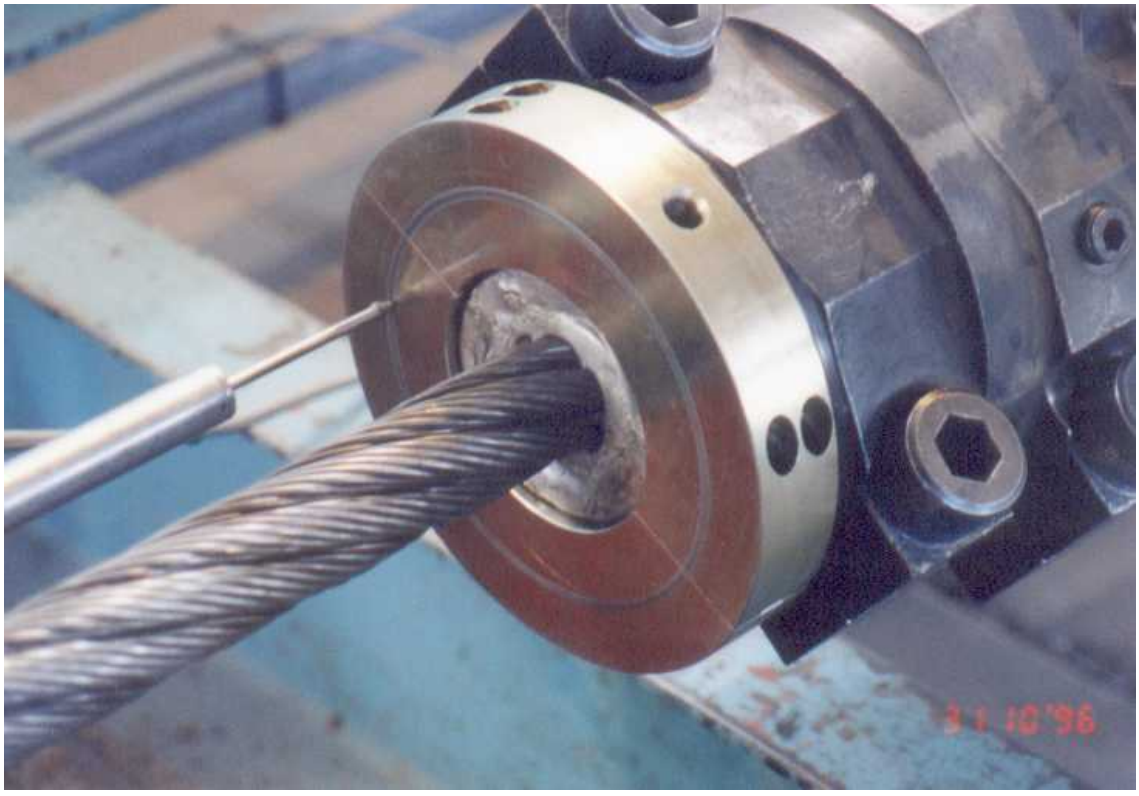

Figure 3.9 - Rotation end, LVDT configuration. The LVDT plunger is sprung to follow the rotating split collar clamp surface (galvanised annular assembly in the centre).

For constant end rotations, the elongation measurement is used to determine rope modulus. The LVDT on the rotation end is sprung and the nib follows the movement of the split collar clamp, figure 3.9. On the cylinder end a magnet is used to connect the LVDT plunger to the clamp. Accurate measurement of the rope end rotation is achieved with an optical shaft encoder fitted to the first stage (shaft) of the reduction chain drive as shown in figure 3.10.

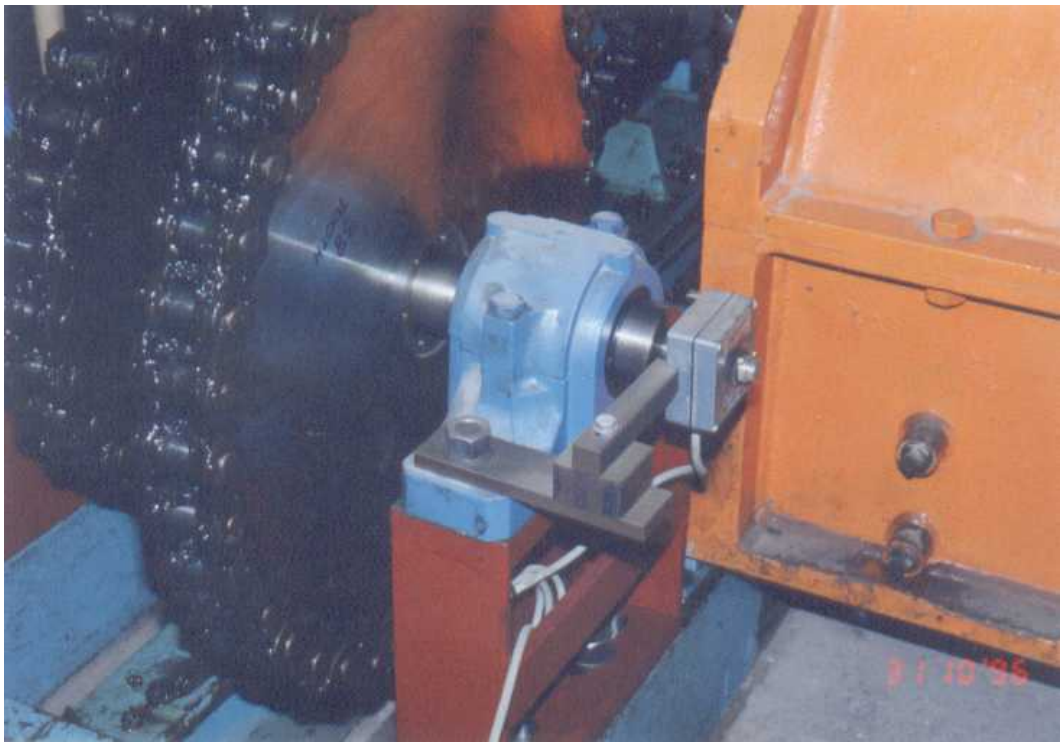

Figure 3.10 - Optical shaft encoder for end rotation measurement. The reduction chain drive is to the left and the gearbox to the right.

3.2.5 Diameter and lay length measurement

Two sets of sprung parallel plates, each with two LVDT's, measure the change in rope diameter. The plate sets are mounted perpendicular to one another as shown in figure 3.11. The change in diameter in calculated from the average of the four displacements measured by the LVDT's. The spring force on the plates results in the jig rotating with the rope when the end rotation is varied. For clarity the springs and steel slides, which keep the plate surfaces parallel, are not shown in figure 3.11 but are indicted in figure 3.12. Torsional strains in winding installations result in the alteration of rope strand orientations and therefore rope diameter. Similarly axial loading is accompanied by reductions in rope diameter. The

relationship between the sheave grove radius and rope diameter can affect the in–service endurance of a rope and it is therefore of interest to be able to determine the variation in diameter under the influence of twisting and load.

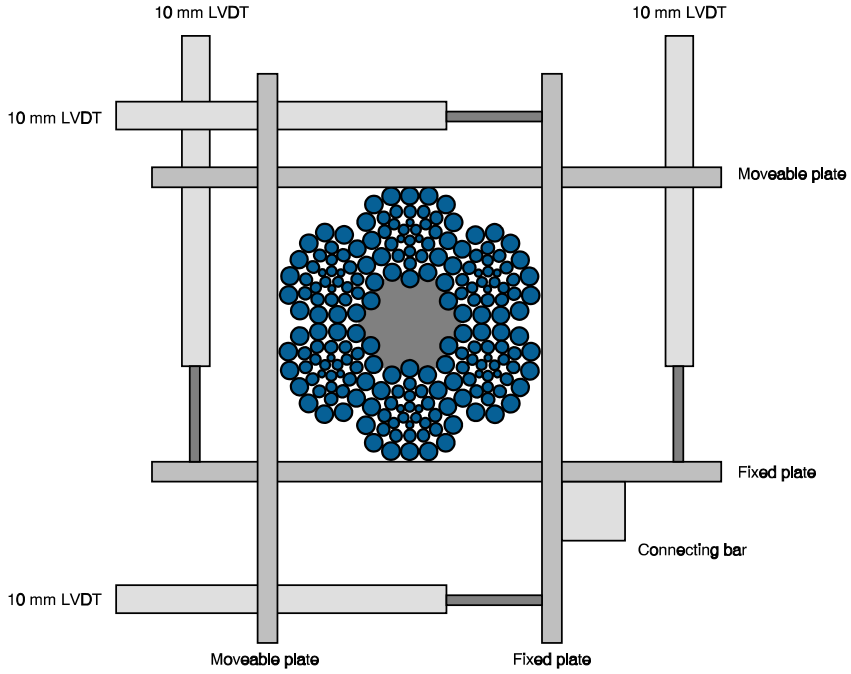

Figure 3.11 - Configuration of the rope diameter measurement jig.

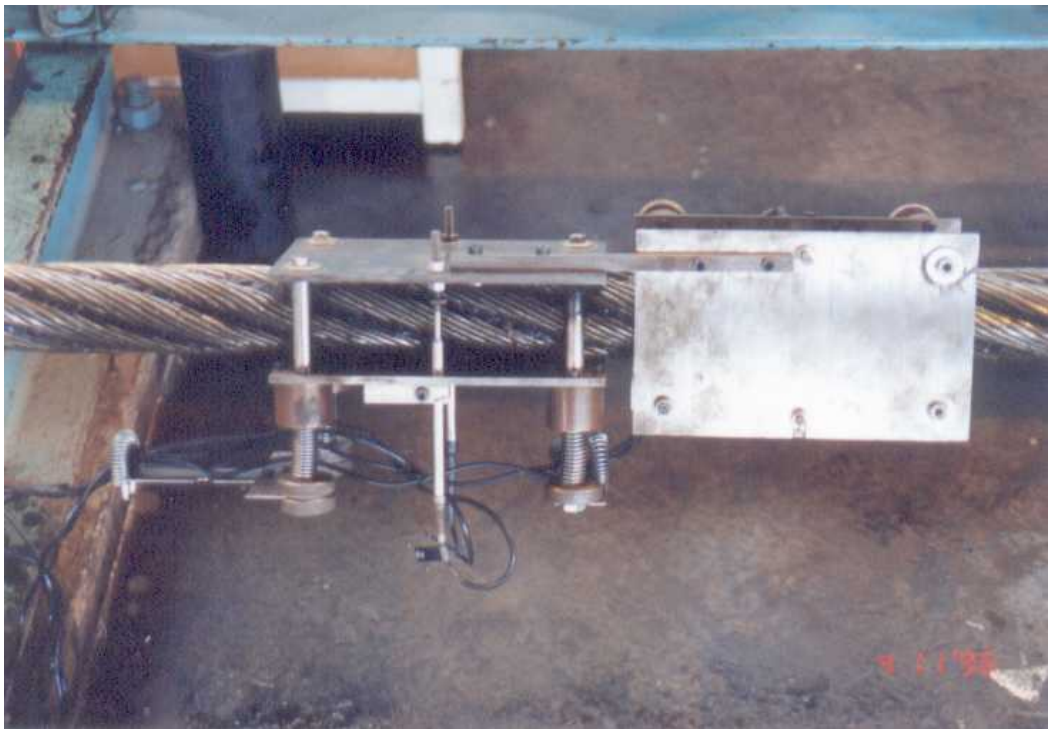

Figure 3.12 - View of the rope diameter measurement jig fitted to a triangular strand rope.

Prior to testing, the rope's zero twist diameter (d_0) is measured with a wide jaw vernier, shown in figure 3.13.

Figure 3.13 - Wide jaw vernier for manual rope diameter measurement.

The strand lay length of a rope specimen is measured manually with a lay length gauge, shown in figures 3.14 and 3.15. The double slide mechanism with the two V-blocks ensures that the lay length is measured parallel to the longitudinal axis of the rope. The pointed screws, through each block, can be adjusted for depth depending on the rope diameter. Once the blocks and screws have been correctly positioned, the lay length is measured across the centre lines of the screws. The use of this type of gauge results in very accurate and repeatable readings for rope lay length. The gauge was designed and manufactured specifically for this study. On a six strand rope it is advisable to measure the lay length over twelve or eighteen strands and divide the result by two or three respectively to further reduce the measurement errors.

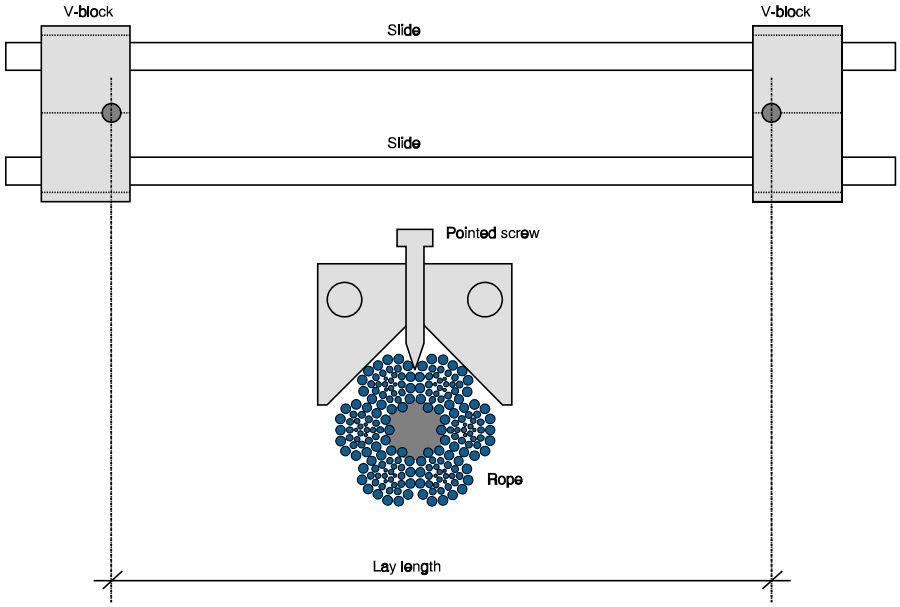

Figure 3.14 - Operation of the parallel V-block lay length measurement gauge.

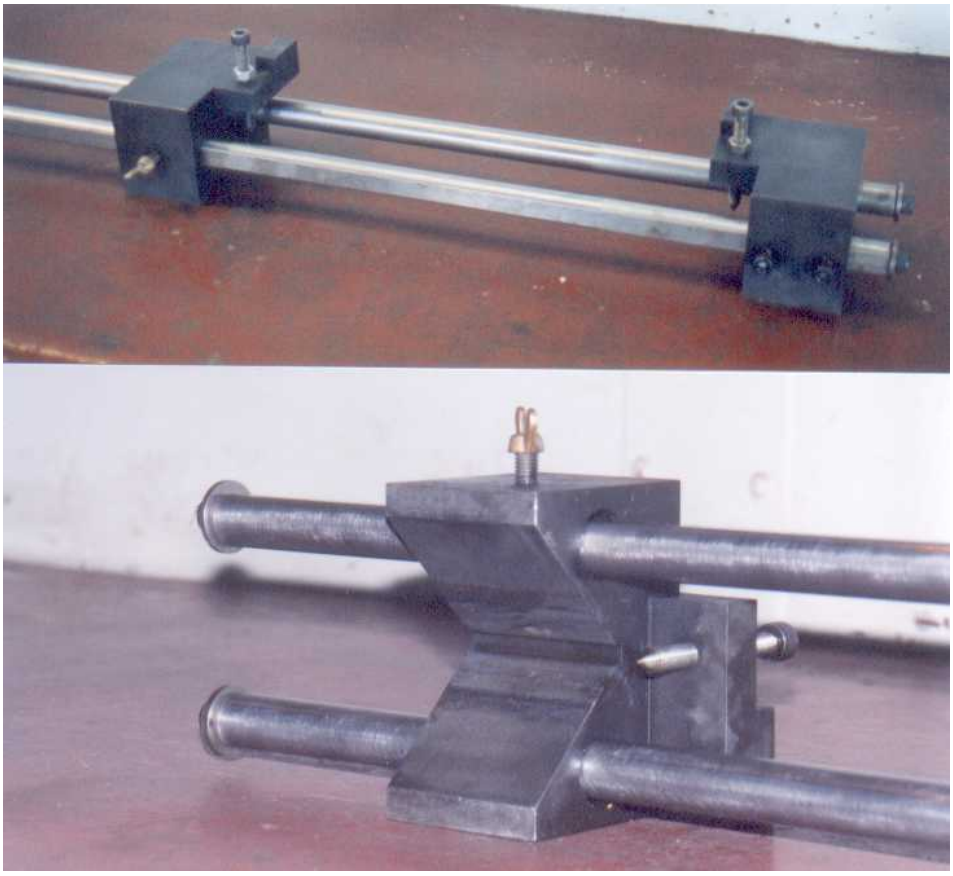

Figure 3.15 - Views of the lay length measurement gauge. A machined, rectangular protrusion on each V-block allows for simple location of the pointed screw centre line.

3.3 Control software

The code for the software is written in Turbo Pascal for MS-DOS®. Figure 3.16 shows the structure of the menu system.

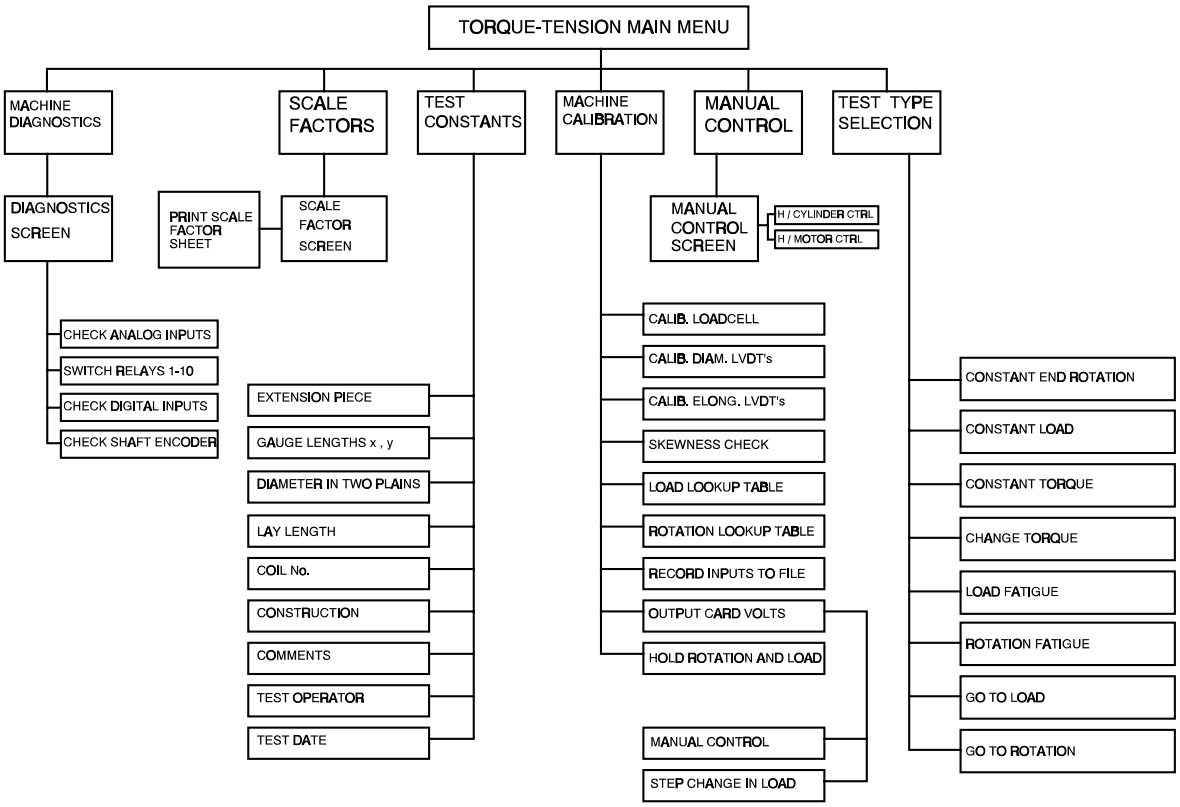

Figure 3.16 - Structure of the testing machine control software menu system.

Diagnostics allows the user to view the input voltages and manually switch the ten PC controlled relays. The digital inputs from the hydraulic cylinder limit switches and the shaft encoder reading can also be monitored from the diagnostics screen.

The scale factors (mechanical units per volt) are determined through automatic calibration procedures and can be printed from the scale factor screen. The values are also saved to an information file for every test data file (*.DAT and *.INF). For each new rope tested, the test constants are entered and are saved to the test information files. If the extension piece is fitted to allow for a shorter rope specimen (2670 mm as opposed to 4040 mm) the software adjusts the fixed length value between the elongation measurement pedestals used to determining the gauge length, figure 3.7.

The calibration menus include automated procedures for in-situ calibration of the measurement instruments. The LVDT's are calibrated using steel blocks and plates of known thicknesses to induce displacements. The motor end split collar clamp skewness factors for the elongation correction (equation [3.2]) can also be determined. The relationship between input voltages to the hydraulic cylinder and motor control cards and the resulting load and rotation speed can be measured and saved as look up tables to data files. As part of diagnostics and fault finding, the input channels can be saved to files without automatic control of the machine taking place. The output control voltages can be varied manually from the keyboard for setting up the hydraulic control cards and determining the load system response to step changes in control voltage. User defined load and rotation values can be maintained by the control PC. Figures 3.17 and 3.18 show how the rope load and rotation head speed vary with changes in the control voltage output from the PC.

Friction in the hydraulic cylinder is considered to be the primary cause of the large hysteresis area associated with the load control. The response shown in figure 3.17 complicates the control since there is a range of voltages associated with a specific load. For example, a 200 kN load could have a control voltage between 6,51 and 7,28 volts. In spite of this limitation it was found that a combination of proportional and integral components in the algorithm ensures adequate levels of control (within ± 3 kN of the control value).

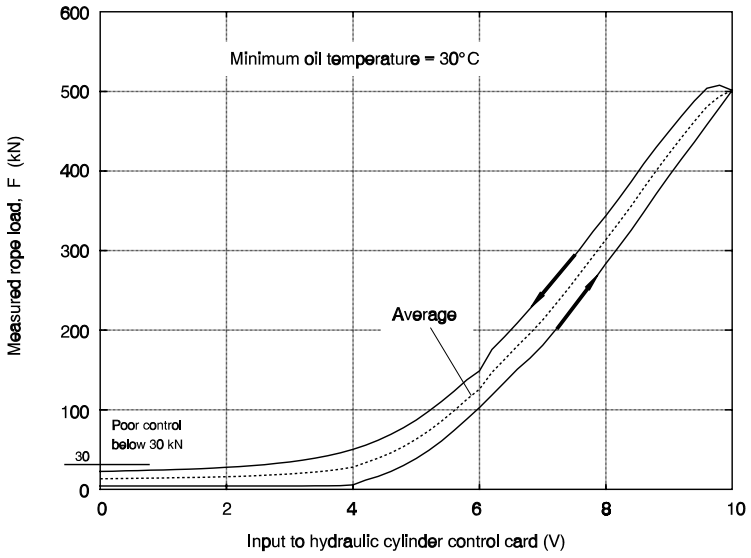

Figure 3.17 - Relationship between the measured load and the control voltage for the hydraulic cylinder. Data for load control look up table.

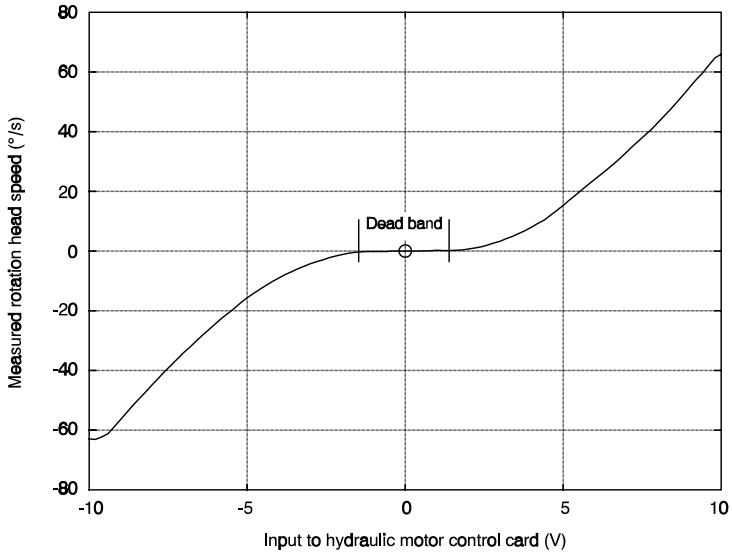

Figure 3.18 - Relationship between the measured rotation head speed and the control voltage for the hydraulic motor. Data for rotation control look up table.

The hydraulic motor is considerably more responsive than the hydraulic cylinder so only a proportional control component is required. For illustration, a procedure which increases the load while maintaining the end rotation constant is listed in figure 3.19. The arctan function for the rotation control reduces the dead band region around the zero output point and limits the maximum output voltage to a predetermined value irrespective of the magnitude of the error. This reduces the likelihood of system instability.

```
Procedure Go_To_Load_Hold_Rot( Rate, Terminal_Load, Rot_Value : real );

repeat
   Check_Time    :=  Read_Time - Start_Time;       { Time since start       }
   Load_Actual   :=  Read_Load;
   Load_Required :=  Start_Load + Rate * Check_Time;
   Load_Error    :=  Load_Actual - Load_Required ;
   I_Part        :=  I_Part + Ic * Load_Error;     { Integral part          }
   Load_Volts    :=  Start_Load_Volts              { Starting CTRL voltage  }
                   + Cc * Check_Time * Rate        { Forcing function       }
                   - Load_Error * Pc               { Proportional CTRL      }
                   - I_Part;                       { Integral CTRL          }
   Pull(Load_Volts);                               { Voltage output         }
                                                   { Ic, Cc, Pc = constants }
   Rot_Actual    :=  Read_Rotation;
   Rot_Error     :=  Rot_Actual - Rot_Value;
   Rot_Volts     :=  -2*arctan(5*Rot_Error);       { Proportional CTRL      }
   Rotate(Rot_Volts);                              { Voltage output         }
until Load_Actual >= Terminal_Load;                { Termination condition  }
```

Figure 3.19 - Example of a load and rotation control algorithm. CTRL = control.

Constant end rotation (≈ constant twist), load and torque tests are conducted from the tests selection screen (figure 3.16). Test parameters are entered by the user in a tabular form as shown in figure 3.20. The software interprets the input parameters and manipulates the machine hardware to achieve the desired results.

```
                CONSTANT ROPE END ROTATION TEST

   Start Rotation          (°)     : -1000.00
   Number of Increments            :    10.00
   Rotation Increment      (°)     :   200.00
   Load End Point          (kN)    :   450.00
   Rate of Load            (kN/s)  :    10.00
   Rate of Data Capture    (Hz)    :     0.80
   No of Bedding In Cycles         :     2.00
   Measure Lay Lengths     (Y/N)   : N
   File Name for Results           : C:\TESTS\CR_TEST.DAT

   Press ESC when finished ....

   Press ESC    to return to the TEST MENU.
   Press ENTER  to start the test.
   Press SPACE  to change the values.
```

Figure 3.20 - Example of constant end rotation test parameter input screen.

In addition to the constant load, torque and twist tests, it is possible to alter the rope torque at constant loads and conduct rotation and load cycles (sinusoidal) at constant load and end rotations respectively. Tests where changes in load and rotation are made without controlling the other parameters can also be conducted.

3.4 Examples of test variable control

Figures 3.21 to 3.23 depict the time based variations in load, twist and torque for the constant twist, load and torque tests. Similar data for load and rotation cycle tests are shown in figures 3.24 and 3.25. The rope used for the tests was a 40 mm, 6x28(10/12/6 + 3Δ), right Lang's lay, of triangular strand construction with 1900 MPa tensile grade wires. The zero twist gauge length was 2676 mm. The first example is for a constant end rotation test, the parameters of which correspond to the operator inputs in figure 3.20. In the case where bedding in cycles are requested, they are executed in between the main loading cycles but are not recorded in the data files. The purpose of the bedding in cycles is to improve repeatability of the test results, allowing the construction to settle down after the change in twist. Note that in all of the five figures which follow, the values shown are those actually measured during the tests.

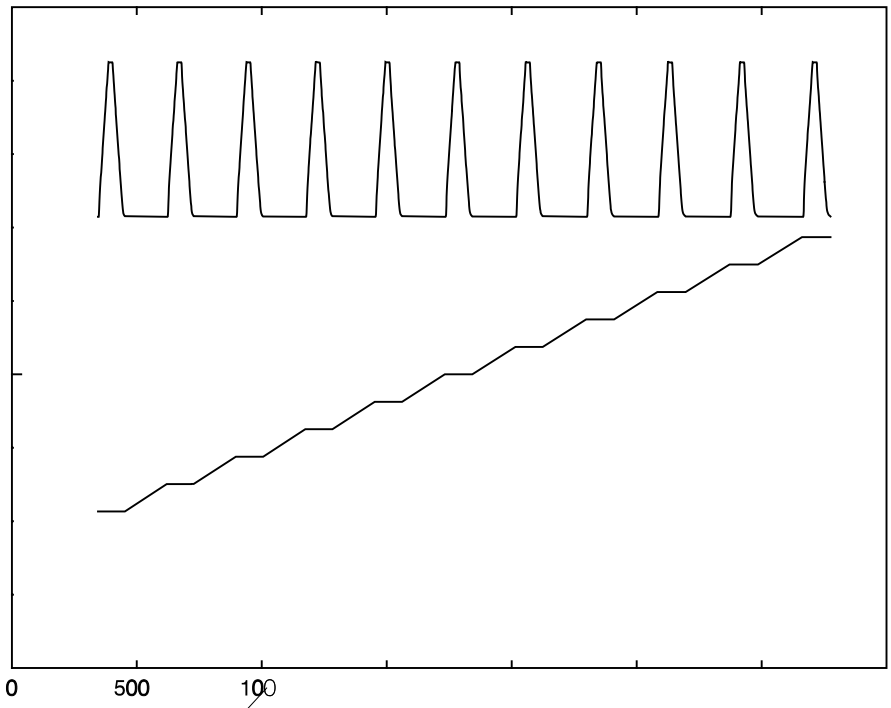

Figure 3.21 - Constant end rotation (twist) test, parameter variations with time.

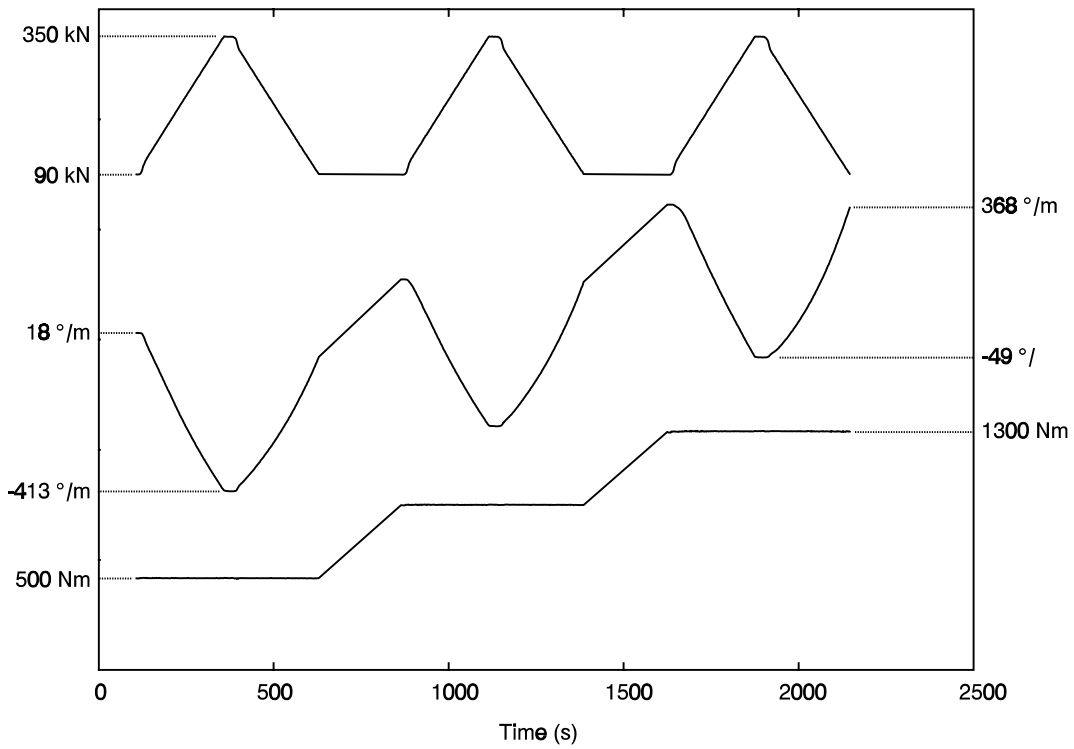

Figure 3.23 - Constant torque test, parameter variations with time.